Effect of Conformational Constraints on Gated Electron-Transfer Kinetics. 3. Copper(II/I) Complexes with *cis*- and *trans*-Cyclopentanediyl-1,4,8,11-tetrathiacyclotetradecane[1]

Prabodha Wijetunge,[2a] Chandrika P. Kulatilleke,[2a] Luke T. Dressel,[2b] Mary Jane Heeg,[2a] L. A. Ochrymowycz,[2b] and D. B. Rorabacher*[,2a]

Department of Chemistry, Wayne State University, Detroit, Michigan 48202, and Department of Chemistry, The University of Wisconsin—Eau Claire, Eau Claire, Wisconsin 54701

Received January 27, 2000

Previous kinetic and electrochemical studies of copper complexes with macrocyclic tetrathiaethers—such as 1,4,8,-11-tetrathiacyclotetradecane ([14]aneS$_4$)—have indicated that electron transfer and the accompanying conformational change occur sequentially to give rise to a dual-pathway mechanism. Under appropriate conditions, the conformational change itself may become rate-limiting, a condition known as "gated" electron transfer. We have recently hypothesized that the controlling conformational change involves inversion of two donor atoms, which suggests that "gated" behavior should be affected by appropriate steric constraints. In the current work, two derivatives of [14]aneS$_4$ have been synthesized in which one of the ethylene bridges has been replaced by either *cis*- or *trans*-1,2-cyclopentane. The resulting copper systems have been characterized in terms of their $Cu^{II/I}L$ potentials, the stabilities of their oxidized and reduced complexes, and their crystal structures. The electron self-exchange rate constants have been determined both by NMR line-broadening and by kinetic measurements of their rates of reduction and oxidation with six or seven counter reagents. All studies have been carried out at 25 °C, $\mu = 0.10$ M ($NaClO_4$ and/or $Cu(ClO_4)_2$), in aqueous solution. Both Cu(II/I) systems show evidence of a dual-pathway mechanism, and the electron self-exchange rate constants representative of both mechanistic pathways have been determined. The first-order rate constant for gated behavior has also been resolved for the Cu^I(*trans*-cyclopentane-[14]aneS$_4$) complex, but only a limiting value can be established for the corresponding *cis*-cyclopentane system. The rate constants for both systems investigated in this work are compared to values previously determined for the Cu(II/I) systems with the parent [14]aneS$_4$ macrocycle and its derivatives involving phenylene and *cis*- or *trans*-cyclohexane substituents. The results are discussed in terms of the influence of the fused rings on the probable conformational changes accompanying the electron-transfer process.

Introduction

Electron transfer in copper(II/I) systems involves an unusually large change in coordination geometry. Copper(II) complexes generally exist as Jahn−Teller distorted five- (square pyramidal) or six-coordinate (tetragonal) species, while copper(I) complexes are predominantly four-coordinate tetrahedral species. In a series of studies,[1,3−11] we have shown that the change in conformation can itself become rate-limiting under specific circumstances so that the reactions become first order, independent of the counter reagent—a condition known as "gated" electron transfer. When this limiting condition is reached, further increases in the reaction driving force may result in a switch to an alternative mechanistic path so that the overall mechanism can be described as a dual-pathway square scheme as depicted in Figure 1.[11] In this scheme, $Cu^{II}L(O)$ and $Cu^{I}L(R)$ (L = a multidentate ligand) are the thermodynamically stable species while $Cu^{II}L(Q)$ and $Cu^{I}L$-(P) are metastable intermediates in which the coordination geometry more nearly resembles that of the thermodynamically stable species of the opposite oxidation state. The general behavior of square scheme systems of this type has been theoretically characterized by Hoffman and Ratner[12] and by Brunschwig and Sutin.[13] (As noted by the latter authors, under appropriate conditions a diagonal pathway is also possible in which conformational change and the electron-transfer step are entirely concerted; however, the appearance of gated behavior indicates that the activation energy for a concerted pathway is greater than for the stepwise pathways involving metastable intermediates.)

Recently, other investigators have also reported observing the onset of gated electron-transfer kinetics in low molecular weight

* To whom correspondence should be addressed. E-mail: dbr@chem.wayne.edu. Fax: (313) 577-1377.

(1) Preceding paper in this series: Dunn, B. C.; Ochrymowycz, L. A.; Rorabacher, D. B. *Inorg. Chem.* **1997**, *36*, 3253−3257.
(2) (a) Wayne State University. (b) University of Wisconsin—Eau Claire.
(3) Bernardo, M. M.; Robandt, P. V.; Schroeder, R. R.; Rorabacher, D. B. *J. Am. Chem. Soc.* **1989**, *111*, 1224−1231.
(4) Meagher, N. E.; Juntunen, K. L.; Heeg, M. J.; Salhi, C. A.; Ochrymowycz, L. A.; Rorabacher, D. B. *J. Am. Chem. Soc*. **1992**, *114*, 10411−10420.
(5) Robandt, P. V.; Schroeder, R. R.; Rorabacher, D. B. *Inorg. Chem.* **1993**, *32*, 3957−3963.
(6) Leggett, G. H.; Dunn, B. C.; Vande Linde, A. M. Q.; Ochrymowycz, L. A.; Rorabacher, D. B. *Inorg. Chem.* **1993**, *32*, 5911−5918.
(7) Meagher, N. E.; Juntunen, K. L.; Salhi, C. A.; Dunn, B. C.; Ochrymowycz, L. A.; Rorabacher, D. B. *Inorg. Chem.* **1994**, *33*, 670−679.
(8) Dunn, B. C.; Ochrymowycz, L. A.; Rorabacher, D. B. *Inorg. Chem.* **1995**, *34*, 1954−1956.
(9) Salhi, C. A.; Yu, Q.; Heeg, M. J.; Villeneuve, N. M.; Juntunen, K. L.; Schroeder, R. R.; Ochrymowycz, L. A.; Rorabacher, D. B. *Inorg. Chem.* **1995**, *34*, 6053−6064.
(10) Villeneuve, N. M.; Schroeder, R. R.; Ochrymowycz, L. A.; Rorabacher, D. B. *Inorg. Chem.* **1997**, *36*, 4475−4483.
(11) Martin, M. J.; Endicott, J. F.; Ochrymowycz, L. A.; Rorabacher, D. B. *Inorg. Chem.* **1987**, *26*, 3012−3020.
(12) Hoffman, B. M.; Ratner, M. A. *J. Am. Chem. Soc.* **1987**, *109*, 6237−6243. Correction: *J. Am. Chem. Soc.* **1988**, *110*, 8267.
(13) Brunschwig, B. S.; Sutin, N. *J. Am. Chem. Soc.* **1989**, *111*, 7454−7465.

10.1021/ic0000909 CCC: $19.00 © 2000 American Chemical Society
Published on Web 06/06/2000

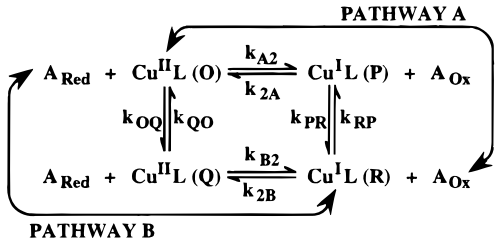

Figure 1. Dual-pathway square scheme mechanism proposed for Cu(II/I) electron-transfer reactions. Species $Cu^{II}L(O)$ and $Cu^{I}L(R)$ represent the stable forms of the oxidized and reduced complexes, respectively, while $Cu^{II}L(Q)$ and $Cu^{I}L(P)$ represent corresponding metastable intermediates. Species A_{Red} and A_{Ox} represent counter reagents. The horizontal reactions involve electron transfer, while the vertical reactions involve conformational rearrangements of the copper complexes. Under conditions where one of the conformational steps becomes rate-limiting, the overall reaction becomes independent of reagent concentration and the reaction is said to be "gated".

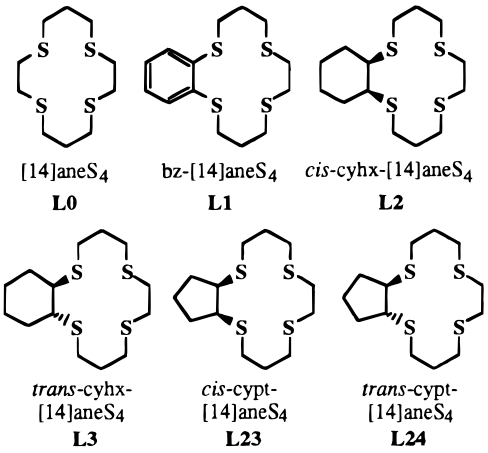

Figure 2. Ligands discussed in this work.

Cu(II/I) systems. Takagi and co-workers have observed gated electron transfer in Cu(II/I) systems involving substituted phenanthroline ligands.[14] Stanbury, Wilson, and co-workers[15] have identified one system that appears to exhibit gated kinetics for the electron self-exchange process itself on the basis of the fact that the $Cu^{I}L$ NMR spectrum showed no line broadening as the $Cu^{II}L$ concentration was increased. However, such behavior would also occur if the self-exchange process were too slow for the NMR time scale.

On the basis of a combination of molecular mechanical calculations and rapid-scan cyclic voltammetric measurements,[3,5,10,16] we have recently proposed that the conformational changes (O ⇌ Q or R ⇌ P) in macrocyclic tetrathiaether complexes may be regulated by the rate of inversion of two donor atoms.[10] The rate constant for these conformational changes, in turn, should be sensitive to restrictions in the flexibility of the macrocyclic ligand in the vicinity of the donor atoms themselves. In the two previous papers in the current series, we have studied the electron-transfer kinetic behavior of Cu(II/I) complexes formed with derivatives of 1,4,8,11-tetrathiacyclotetradecane ([14]aneS$_4$) in which *cis*- or *trans*-1,2-cyclohexane (L2 and L3)[9] or 1,2-phenylene (L1)[1] has been substituted for one of the ethylene bridges (see Figure 2) and have contrasted their behavior with that of the parent Cu(II/I) system involving unsubstituted [14]aneS$_4$ (L0).

In the current work we have extended our measurements to include the electron-transfer kinetics of Cu(II/I) systems in which *cis*- or *trans*-1,2-cyclopentane (L23 and L24 in Figure 2)[17] has been substituted for one of the ethylene bridges in [14]aneS$_4$. This study was predicated on the fact that cyclopentane rings are more rigid than cyclohexane rings and yet exhibit the same inductive effects on the sulfur donor atoms. Thus, it was hypothesized that a comparison of the kinetic behavior exhibited by the corresponding cyclopentane and cyclohexane derivatives might make it possible to distinguish the influence of decreased macrocyclic flexibility on the kinetics of conformational change without introducing other factors.

Experimental Section

Ligand Syntheses. The synthetic route utilized to generate the cyclopentanediyl ligands, L23 and L24, is formally analogous to that described previously for the corresponding phenylene (L1) and cyclohexanediyl (L2 and L3) derivatives of [14]aneS$_4$ (L0).[18] The general approach involves (i) condensation of *cis*- or *trans*-1,2-cyclopentanedithiol with 2 equiv of 3-chloropropanol to afford the corresponding *cis*- or *trans*-1,2-bis((3-hydroxypropyl)thio)cyclopentanes, (ii) conversion of the alcohol derivatives to the corresponding 1,2-bis((3-chloropropyl)thio)cyclopentanes, and (iii) high-dilution cyclocondensation of the chloro derivatives with 1,2-ethanedithiol. It should be noted that several attempts to prepare these ligands by the seemingly simpler design strategy of high-dilution cyclocondensation of the *cis*- or *trans*-1,2-cyclopentanedithiols with 1,10-dichloro-4,7-dithiadecane resulted overwhelmingly in intrachain cyclization to 7- and 11-membered di- and trithiamesocyclic products. These products are only minor byproducts in the preferred scheme.

***cis*- and *trans*-1,2-Cyclopentanedithiol.** Literature methods for preparing the *cis*- and *trans*-cyclopentanedithiols[19] failed to yield significant isomerically pure product. We were able to prepare *cis*-1,2-cyclopentanedithiol in over 40% yield through the analogous four-step process previously developed for *cis*-1,2-cyclohexanedithiol.[18] The only modification required was that the oxidative conversion of cyclopentene to *cis*-1,2-cyclopentane bisacetate was performed below 40 °C, taking into consideration the lower boiling point of cyclopentene.

The synthesis of *trans*-1,2-cyclopentanedithiol has been traditionally achieved through lithium aluminum hydride (LAH) reduction of *trans*-1,2-cyclopentanedithiol tricarbonate. However, we were unable to achieve a significant yield of the tricarbonate.[20] Thus, we devised an alternative method in which cyclopentene oxide (Aldrich Chemical Co.) was converted to cyclopentene sulfide in greater than 80% yield by an effective literature method.[21] Antiaddition of H_2S to the cyclopentane sulfide to afford *trans*-1,2-cyclopentanedithiol was achieved as described below.

A magnetically stirred, ice-cooled, 1 L three-necked flask was fitted with a nitrogen atmosphere sweep adapter, immersion thermometer, and a Claisen adapter for reagent addition and gas-venting through a Friedrich condenser into an oil bubbler. The flask was charged with 600 mL of methanol and 5 mL of concentrated HCl, then saturated

(14) (a) Koshino, N.; Kuchiyama, Y.; Ozaki, H.; Funahashi, S.; Takagi, H. D. *Inorg. Chem.* **1999**, *38*, 3352−3360. (b) Koshino, N.; Kuchiyama, Y.; Funahashi, S.; Takagi, H. D. *Chem. Phys. Lett.* **1999**, *306*, 291−296. (c) Koshino, N.; Kuchiyama, Y.; Funahashi, S.; Takagi, H. D. *Can. J. Chem.* **1999**, *77*, 1498−1507.

(15) Flanagan, S.; Dong, J.; Haller, K.; Wang, S.; Scheidt, W. R.; Scott, R. A.; Webb, T. R.; Stanbury, D. M.; Wilson, L. J. *J. Am. Chem. Soc.* **1997**, *119*, 8857−8868.

(16) Robandt, P. V.; Schroeder, R. R.; Rorabacher, D. B. *Inorg. Chem.* **1993**, *32*, 3957−3963.

(17) The numbers assigned to the ligands are contiguous with assignments given to related compounds reported in previous publications (see refs 18 and 25).

(18) Aronne, L.; Dunn, B. C.; Vyvyan, J. R.; Souvignier, C. W.; Mayer, M. J.; Howard, T. A.; Salhi, C. A.; Goldie, S. N.; Ochrymowycz, L. A.; Rorabacher, D. B. *Inorg. Chem.* **1995**, *34*, 357−369.

(19) Willett, J. D.; Grunwell, J. R.; Berchtold, G. A. *J. Org. Chem.* **1968**, *33*, 2297−2302 and references therein.

(20) Iqbal, S. M.; Owen, L. N. *J. Chem. Soc.* **1960**, 1030−1036.

(21) Goodman, L.; Benitez, A.; Baker, B. R. *J. Am. Chem. Soc.* **1958**, *80*, 1680−1686.

with H_2S through a fritted glass dispersion tube from a gas cylinder. Under nitrogen atmosphere, to the cold solution was added dropwise 31 g (0.31 mol) of cyclopentene sulfide dissolved in 50 mL of methanol. After sulfide addition, the ice cold solution was vigorously purged with a through-liquid stream of nitrogen to expel most of the excess H_2S. The solution was poured into a liter of ice water and extracted with 3 × 200 mL of pentane. The combined pentane extracts were dried with $MgSO_4$, filtered, and concentrated by rotary vacuum evaporation below 30 °C/18 Torr. The residue oil was vacuum-distilled at 68−75 °C/10−13 Torr to afford 32 g (77%) of GC−MS pure product identical to an authentic sample. The pot residue was characterized as consisting of higher molecular weight dithiols with sulfide condensation products.

***cis*- and *trans*-1,2-Bis((3-hydroxypropyl)thio)cyclopentanes.** A 1 L mantle-heated, magnetically stirred, three-necked flask was fitted with an argon gas inlet adapter, pressure-equalizing dropper funnel, and a Friedrich condenser through which the argon gas sweep was vented to an oil bubbler at about 3 mL min^{-1}. The flask was charged with 500 mL of absolute ethanol into which was dissolved 24.4 g (0.42 mol) of KOH pellets. A solution of *trans*-1,2-cyclopentanedithiol, 26.8 g (0.2 mol) in 50 mL of ethanol, was added all at once, and the mildly exothermic solution was allowed to cool for about an hour. To this dimercaptide solution was added dropwise a solution of 3-chloropropanol, 42.5 g (0.45 mol) in 50 mL of ethanol. After addition of reactants, the vigorously stirred salt suspension was brought to reflux, then cooled to ice bath temperature. Precipitated KCl was separated by vacuum filtration and the ethanolic filtrate concentrated by rotary vacuum evaporation. The residue of oil and suspended salt was dispersed in 400 mL of water and extracted with 3 × 100 mL portions of methylene chloride, dried with $MgSO_4$, and concentrated by rotary vacuum evaporation below 45 °C/18 Torr to yield 47.5 g (95%) of product as a colorless oil. Spectroscopic analysis established that the product was essentially pure and suitable for direct use. (It should be noted that attempted distillation of a prior sample by Kugelrohr distillation, 140−155 °C/0.05 Torr, resulted in considerable decomposition.) ^{13}C NMR (100.6 MHz, $CDCl_3$), δ in ppm (multiplicity): 23.60 (t), 28.32 (t), 32.19 (t), 50.57 (d), 60.91 (t). EI-MS, *m*/*e* (relative intensity): 250 M^+ (0.8), 159 (45), 158 (60), 67 (100).

In identical fashion, *cis*-1,2-cyclopentanedithiol was converted on a 0.2 mol scale to the corresponding *cis*-1,2-bis((3-hydroxypropyl)thio)-cyclopentane in 93% yield, isolated as an essentially pure, colorless oil product by rotary vacuum evaporation of extraction solvent. ^{13}C NMR (100.6 MHz, $CDCl_3$), δ in ppm (multiplicity): 24.18 (t), 28.50 (t), 31.33 (t), 31.75 (t), 50.98 (d), 61.38 (t). EI-MS, *m*/*e* (relative intensity): 250 M^+ (1.5), 191 (8), 159 (35), 158 (70), 67 (100).

***cis*- and *trans*-1,2-Bis((3-chloropropyl)thio)cyclopentanes.** In the same apparatus design employed above, 25 g (0.1 mol) of the *trans*-1,2-bis((3-hydroxypropyl)thio)cyclopentane dissolved in 500 mL of dry methylene chloride was reacted with dropwise addition of 25 g (0.21 mol) of thionyl chloride in 75 mL of methylene chloride under a 5 mL min^{-1} argon sweep to expel byproducts HCl and SO_2. The reaction was brought to gentle reflux for one-half hour after reagent addition and then cooled, and solvent was removed by rotary vacuum evaporation below 40 °C at 20 Torr. The residue, a pale-brown oil, was then subjected to further Kugelrohr evaporation at room temperature, 0.1 Torr, for an hour to remove any remaining volatiles. Attempted vacuum distillation, and even prolonged cold storage, results in extensive decomposition. The freshly prepared product was isolated essentially pure and suitable for immediate use in nearly quantitative yield, 28.5 g. ^{13}C NMR (100.6 MHz, $CDCl_3$), δ in ppm (multiplicity): 23.61 (t), 28.88 (t), 32.20 (t), 33.19 (t), 43.56 (d), 50.72 (t). EI-MS, *m*/*e* (relative intensity): 286 M^+ (3), 177 (4), 99 (35), 67 (100).

In similar fashion, 0.1 mol of *cis*-1,2-bis((3-hydroxypropyl)thio)-cyclopentane afforded 27.3 g (95.5%) of *cis*-1,2-bis((3-chloropropyl)-thio)cyclopentane. ^{13}C NMR (100.6 MHz, $CDCl_3$), δ in ppm (multiplicity): 22.88 (t), 28.57 (t), 32.49 (t), 32.49 (t), 33.09 (t), 41.55 (d), 50.75 (t). EI-MS, *m*/*e* (relative intensity): 286 M^+ (2), 209 (6), 177 (65), 99(40), 67 (100).

***cis*- and *trans*-2,3-Cyclopentano-1,4,8,11-tetrathiacyclotetradecanes.** The apparatus design previously described[18] was employed except for the following modification for reaction scale as documented first for the *trans*-cyclopentyl derivative. A 2 L flask was charged with 1.2 L of anhydrous DMF and 0.21 mol of anhydrous powdered Cs_2CO_3. Programmable HPLC pump addition of an equimolar, 0.09 mol, solution of 1,2-ethanedithiol and *trans*-1,2-bis((3-chloropropyl)thio)-cyclopentane in 300 mL of DMF was carried out at an addition rate of 0.4 mL min^{-1} and dilution pool temperature of 65−70 °C. After the usual workup, the crude product was recovered from 500 mL of methylene chloride extracts as a pale-yellow oil, 26.5 g. Thin-layer chromatography (TLC) analysis of this residue (3:97 ethyl acetate/toluene) showed the major product component at $R_f = 0.45$. This was preceded by byproducts that were subsequently identified by separation and structural characterization to be due to intrachain cyclization including *trans*-2,3-cyclopentano-1,4-dithiacycloheptane ($R_f = 0.88$) and *trans*-2,3-cyclopentano-1,4,8-trithiacycloundecane ($R_f = 0.70$). Elution chromatography through a 2.5 × 60 cm silica gel column, 70:30 cyclohexane/toluene, afforded 11.8 g of combined elution fractions of the major component separated from the more mobile byproducts and higher polymers. After charcoal treatment in 300 mL of hot cyclohexane, the residue was twice recrystallized from 200 mL of 50:50 pentane/hexane to afford 6.95 g (25%) of analytically pure *trans*-2,3-cyclopentano-1,4,8,11-tetrathiacyclotetradecane (L24), mp = 75−76 °C. ^{13}C NMR (100.6 MHz, $CDCl_3$), δ in ppm (multiplicity): 21.45 (t), 29.84 (t), 29.98 (t), 30.70 (t), 31.48 (t), 31.82 (t), 50.33 (d). FT-IR (KBr), ν in cm^{-1} (relative intensity): 2951 (s), 2925 (s), 2857 (m), 1440 (s), 1425 (m), 1302 (w), 1291 (m), 1271 (m), 1247 (m), 1197 (m), 695 (m). EI-MS, *m*/*e* (relative intensity): 308 M^+ (30), 133 (20), 106 (100), 67 (35). Anal. Calcd for $C_{13}H_{24}S_4$: C, 50.64; H, 7.85. Found: C, 50.55; H, 7.90.

In identical fashion on the same reaction scale, the cis isomer was prepared from *cis*-1,2-bis((3-chloropropyl)thio)cyclopentane and 1,2-ethanedithiol. The crude pale-yellow product, 23.75 g, showed TLC components at $R_f = 0.75$, 0.55, and 0.35 (3:97 ethyl acetate/toluene). Elution column chromatography as for the trans isomer yielded 9.2 g of separated major product, which after charcoal treatment, cyclohexane, and three recrystallizations from 150 mL of hexane afforded 4.83 g (17.4%) of analytically pure *cis*-2,3-cyclopentano-1,4,8,11-tetrathiacyclotetradecane (L23), mp = 71−72 °C. ^{13}C NMR (100.6 MHz, $CDCl_3$), δ in ppm (multiplicity): 23.59 (t), 30.00 (t), 31.42 (t), 50.33 (d). FT-IR (KBr), ν in cm^{-1} (relative intensity): 2940 (s), 2872 (s), 1448 (s), 1427 (m), 1413 (m), 1261 (s), 1247 (m), 1190 (m), 696 (m). EI-MS, *m*/*e* (relative intensity): 308 M^+ (25), 133 (20), 106 (100), 67 (40). Anal. Calcd for $C_{13}H_{24}S_4$: C, 50.64; H, 7.85. Found: C, 50.50; H, 7.77.

Other Reagents. The preparation of pure $Cu(ClO_4)_2$ and $NaClO_4$ has been previously described.[22] (WARNING: *Perchlorate salts are potentially explosive! They should not be dried and should be handled with care in small quantities.*) All counter reagents were prepared according to literature methods or modifications thereof as previously reported.[4] The concentrations of counter reagent solutions were determined spectrophotometrically. Clean copper shot, used to reduce $Cu^{II}L$ complexes prior to $Cu^{I}L$ oxidation studies, was prepared as described elsewhere.[4] Standard solutions of $Cu(ClO_4)_2$ and $Hg(ClO_4)_2$ were standardized by titration against EDTA. Ligand solutions were standardized by mole ratio plots in which a large excess of Cu(II) was added to the ligand, and a standard solution of Hg(II) was then added incrementally to displace Cu(II) from the ligand, the disappearance of $Cu^{II}L$ being monitored spectrophotometrically using the strong S → Cu charge-transfer band at approximately 390 nm. Distilled−deionized water was used for the preparation of all solutions. The ionic strength was maintained at 0.10 M using $NaClO_4$ and/or $Cu(ClO_4)_2$.

Crystal Structures. Crystals of $[Cu^{II}(L23)(H_2O)](ClO_4)_2$ and $[Cu^{II}(L24)(H_2O)](ClO_4)_2$ were grown by evaporation from aqueous solutions containing a large excess of $Cu(ClO_4)_2$. For the reduced complexes, a 1:2 ratio of $Cu(ClO_4)_2$ to ligand was dissolved in acetonitrile and reduced over copper shot to generate stoichiometric solutions of $Cu^{I}(L23)$ and $Cu^{I}(L24)$. These solutions were then evaporated slowly in the presence of copper shot. The former crystallized as polymeric $\{[Cu^{I}(L23)]ClO_4\}_x$, whereas $[Cu^{I}(L24)]ClO_4$ was obtained as a monomeric complex. Diffraction data for all four crystals were collected

(22) Diaddario, L. L., Jr.; Ochrymowycz, L. A.; Rorabacher, D. B. *Inorg. Chem.* **1992**, *31*, 2347−2353.

Table 1. Absorbance Peaks, Potentials, and Stability Constants of the Copper Complexes with the *cis*- and *trans*-Cyclopentanediyl Derivatives of [14]aneS$_4$, and Related Systems, As Determined at 25 °C, $\mu = 0.10$ M

complexed ligand	λ_{max}, nm	$10^{-3}\epsilon_{Cu^{II}L}$, M^{-1} cm^{-1}	E^f, V vs SHE[a]	$10^{-4}K_{Cu^{II}L}$, M^{-1}	$10^{-13}K_{Cu^{I}L}$, M^{-1} (calcd)
[14]aneS$_4$ (L0)	390, 575[b]	8.04, 1.9[b,c]	0.59[d]	2.18[c] [0.300][e,f]	0.1
bz-[14]aneS$_4$ (L1)	[382, ~564][e,f]		~0.84[g]	[~0.001][e,f]	
cis-cyhx-[14]aneS$_4$ (L2)	390, 570[f]	7.4, 2.0[f]	0.536[f]	~110 [16.1][e,f]	[0.63][e,f]
trans-cyhx-[14]aneS$_4$ (L3)	388, 558[f]	8.9, 1.8[f]	0.600[f]	~80 [11.2][e,f]	[2.5][e,f]
cis-cypt-[14]aneS$_4$ (L23)	391, 570[h]	7.0, 1.98[h]	0.560[h]	23[h]	40[h]
trans-cypt-[14]aneS$_4$ (L24)	394, 575[h]	7.8, 1.6[h]	0.670[h]	0.30[h]	40[h]

[a] Half-wave potentials from slow-scan aqueous cyclic voltammetry corrected to SHE (based on ferroin as the external reference for which $E^f = 1.112$ V [refs 24 and 11]). [b] Jones, T. E.; Rorabacher, D. B.; Ochrymowycz, L. A. *J. Am. Chem. Soc.* **1975**, *97*, 7485−7486. [c] Reference 27. [d] Bernardo, M. M.; Schroeder, R. R.; Rorabacher, D. B. *Inorg. Chem.* **1991**, *30*, 1241−1247. [e] Bracketed values are in 80% methanol; aqueous estimates of $K_{Cu^{II}L}$ for Cu^{II}(L2) and Cu^{II}(L3) are based on the observation that such values are generally about 7 times larger than in 80% methanol. [f] Reference 18. [g] Although Cu$^{II/I}$(L1) is not sufficiently soluble to permit the potential to be determined directly in water, the trend is relatively uniform for this series of ligands regardless of solvent; the aqueous estimate listed is based on $E^f = 0.80$ V for Cu$^{II/I}$(L1) in acetonitrile compared to 0.55 V for Cu$^{II/I}$(L0) in the same medium [ref 18]. [h] This work.

on a Siemens/Bruker P4/CCD diffractometer equipped with monochromated Mo Kα radiation and the manufacturer's SMART collection software and SAINT processing software. A hemisphere of data was collected at 10 s/frame with 0.3° between each frame. Absorption corrections were applied with the program SADABS.[23] The structure was solved and refined on F^2 with the programs *SHELXS* and *SHELXL*-93.[23] Hydrogen atoms were placed in calculated or observed positions. All non-hydrogen atoms were anisotropically described except for some isotropically refined partial atoms in the disordered perchlorate groups.

Instrumentation. Routine ultraviolet and visible spectra were obtained using a Hewlett-Packard 8452A diode array spectrophotometer. Analytical spectrophotometric measurements were carried out using a thermostated Cary model 17 dual-beam spectrophotometer. Cyclic voltammetric measurements were made with a Bioanalytical Systems electrochemical analyzer, model BAS 100 (BAS, West Lafayette, IN). A glassy carbon electrode (BAS) was used as the working electrode to minimize problems of ligand absorption on the electrode surface. A platinum wire auxiliary electrode and a Ag/AgCl reference electrode containing 3 M NaCl (BAS) were also utilized. All potential measurements were made using ferroin ($E^{\circ\prime} = 1.112$ V) as an external standard.[24,25] A Varian Unity 500 NMR spectrometer was used for all line-broadening measurements. All kinetic measurements were made with a Durrum D110 stopped-flow spectrophotometer with Kel-F fittings, equipped with airtight syringes, which was interfaced to a PC. Data analyses were performed using software written in-house. For both the thermodynamic and kinetic measurements the temperature was thermostated at 25.0 ± 0.2 °C.

Results

Stability Constants and Potentials. The formal potential values for both Cu(II/I) systems included in this work were determined for solutions containing a large excess of Cu(II) using cyclic voltammetry at ambient temperature with a scan rate of 25 mV s^{-1}. At this scan rate only one set of peaks was observed with a peak-to-peak separation of 60−63 mV, indicating that the systems were completely reversible. The average $E_{1/2}$ value from several trials was taken as the formal potential for each system, and the resultant values are included in Table 1.

The spectra for the Cu^{II}L complexes with both *cis*- and *trans*-cypt-[14]aneS$_4$ (cypt ≡ cyclopentanediyl) revealed the presence of two intense S → Cu charge-transfer peaks in the visible region as listed in Table 1. The stability constants and molar absorptivities of the Cu^{II}L complexes at 25 °C were determined simultaneously by the method of McConnell and Davidson[26] as previously described[27,28] using the absorbance peak in the vicinity of 390 nm. The resulting values are listed in Table 1.

On the basis of the stability constants of the Cu^{II}L complexes and the redox potentials, the stability constants of the corresponding Cu^{I}L complexes were calculated using the Nernst equation as described earlier.[29] These calculated values are also included in Table 1.

Crystallographic Structural Determinations. The experimental parameters for all four crystal structures are presented in Table 2. ORTEP diagrams of the cationic units of Cu^{II}(L23)(H$_2$O), Cu^{II}(L24)(H$_2$O), [Cu^{I}(L23)]$_x$, and Cu^{I}(L24), showing the atom labeling schemes, are presented in Figures 3−6. Selected bond lengths and bond angles are listed in Table 3. Both of the Cu(II) cationic units (Figures 3 and 4) are seen to be five-coordinate with the copper atom bonded to the four sulfur donor atoms and an apical water molecule. For the complexes with L23 and L24, Cu(II) is situated 0.13 and 0.20 Å, respectively, above the mean plane of the four sulfurs. Both displacements are significantly smaller than the 0.28 Å previously found for Cu(II) in the complexes formed with the corresponding cyclohexane derivatives.[9]

In the cationic unit of Cu^{I}(L23), each copper atom is bonded to two sulfurs from each of two different ligands while the other two sulfur donor atoms from each ligand are bonded to adjacent copper atoms to generate a 2:2 polymer. Figure 5 illustrates the general structure for one macrocyclic ligand and its coordinated copper atoms. A similar 2:2 polymeric crystal structure has been observed previously for the Cu(I) complex of a related acyclic tetrathiaether (3,6,10,13-tetrathiapentadecane);[30] and the crystal structure of Cu^{I}([14]aneS$_4$) revealed a 3:1 polymer, each copper being bonded to three sulfurs of one ligand molecule and one sulfur of a second ligand.[31] In all three cases, however, the oxidation kinetics of Cu^{I}L indicate that the complexes are monomeric in dilute solution.[4,9] For Cu^{I}(L24), a

(23) Sheldrick, G. SHELX-86, SHELXL-93, and SADABS; University of Göttingen: Göttingen, Germany, 1986, 1993, and 1996.
(24) Yee, E. L.; Cave, R. J.; Guyer, K. L.; Tyma, P. D.; Weaver, M. J. *J. Am. Chem. Soc.* **1980**, *101*, 1131−1132.
(25) Ambundo, E. A.; Deydier, M.-V.; Grall, A. J.; Aguera-Vega, N.; Dressel, L. T.; Cooper, T. H.; Heeg, M. J.; Ochrymowycz, L. A.; Rorabacher, D. B. *Inorg. Chem.* **1999**, *38*, 4233−4242.
(26) McConnell, H.; Davidson, N. *J. Am. Chem. Soc.* **1950**, *72*, 3164−3167. Benesi, H. A.; Hildebrand, J. H. *J. Am. Chem. Soc.* **1949**, *71*, 2703−2707.
(27) Sokol, L. S. W. L.; Ochrymowycz, L. A.; Rorabacher, D. B. *Inorg. Chem.* **1981**, *20*, 3189−3195.
(28) Young, I. R.; Ochrymowycz, L. A.; Rorabacher, D. B. *Inorg. Chem.* **1986**, *25*, 2576−2582.
(29) Bernardo, M. M.; Heeg, M. J.; Schroeder, R. R.; Ochrymowycz, L. A.; Rorabacher, D. B. *Inorg. Chem.* **1992**, *31*, 191−198.
(30) Diaddario, L. L., Jr.; Dockal, E. R.; Glick, M. D.; Ochrymowycz, L. A.; Rorabacher, D. B. *Inorg. Chem.* **1985**, *24*, 356−363.
(31) Dockal, E. R.; Diaddario, L. L.; Glick, M. D.; Rorabacher, D. B. *J. Am. Chem. Soc.* **1977**, *99*, 4530−4532.

Table 2. Crystal Parameters and Experimental Data for X-ray Diffraction Measurements on $[Cu^{II}(L23)(H_2O)](ClO_4)_2$, $[Cu^{II}(L24)(H_2O)](ClO_4)_2$, $\{[Cu^{I}(L23)]ClO_4\}_x$, and $[Cu^{I}(L24)]ClO_4$[a]

parameter	$[Cu^{II}(L23)(H_2O)](ClO_4)_2$	$[Cu^{II}(L24)(H_2O)](ClO_4)_2$	$\{[Cu^{I}(L23)]ClO_4\}_x$	$[Cu^{I}(L24)]ClO_4$
empirical formula	$CuC_{13}H_{26}S_4Cl_2O_9$	$CuC_{13}H_{26}S_4Cl_2O_9$	$CuC_{13}H_{24}S_4ClO_4$	$CuC_{13}H_{24}S_4ClO_4$
fw	589.02	589.02	471.55	471.55
space group	$P\bar{1}$	$Pna2_1$	$P2_1/n$	$P2_1$
a, Å	8.2607(2)	16.2369(9)	10.8299(7)	7.3387(9)
b, Å	11.1482(3)	13.6473(8)	16.854(1)	17.969(2)
c, Å	13.0981(3)	10.4642(5)	11.5157(7)	7.4432(9)
α, deg	82.783(1)	90	90	90
β, deg	84.104(1)	90	116.493(1)	97.814(2)
γ, deg	78.000(1)	90	90	90
V, Å^3	1166.87(5)	2318.8(2)	1881.2(2)	972.4(2)
Z	2	4	4	2
ρ_{calcd}, g cm^{-3}	1.676	1.687	1.665	1.611
μ, mm^{-1}	1.564	1.574	1.761	1.703
$R(F)$[b]	0.0417	0.0446	0.0515	0.0564
$R_w(F^2)$[c]	0.1047	0.1192	0.1336	0.1677

[a] $T = 295(2)$ K; $\lambda = 0.710\ 73$ Å. [b] $R(F) = \sum||F_o| - |F_c||/\sum|F_o|$ for $2\sigma(I)$ reflections. [c] $R_w(F^2) = [\sum w(F_o^2 - F_c^2)^2/\sum w(F_o^2)^2]^{1/2}$ for $2\sigma(I)$ reflections.

Table 3. Selected Bond Lengths and Bond Angles for the Cationic Units in the Crystal Structures of $[Cu^{II}(L23)(H_2O)](ClO_4)_2$, $[Cu^{II}(L24)(H_2O)](ClO_4)_2$, $\{[Cu^{I}(L23)]ClO_4\}_x$, and $[Cu^{I}(L24)]ClO_4$

	$Cu^{II}(L23)(H_2O)$	$Cu^{II}(L24)(H_2O)$	$\{Cu^{I}(L23)\}_x$[a]	$Cu^{I}(L24)$
		Bond Lengths (Å)		
Cu−S(1)	2.3028(9)	2.350(2)	2.322(1)	2.292(2)
Cu−S(2)	2.296(1)	2.340(2)	2.299(1)	2.296(2)
Cu−S(3)	2.309(1)	2.312(2)	2.364(1)	2.279(2)
Cu−S(4)	2.329(1)	2.339(2)	2.304(1)	2.267(3)
Cu−O(1)	2.282(3)[b]	2.241(5)[c]		
mean Cu−S	2.31[b]	2.34[c]	2.32	2.28[d]
		Bond Angles (Deg)		
S(1)−Cu−S(2)	88.80(4)	90.18(6)	91.48(4)	95.61(8)
S(2)−Cu−S(3)	94.72(4)[e]	93.39(7)[e]	125.79(5)	111.20(8)
S(3)−Cu−S(4)	88.52(4)	88.86(7)	92.00(5)	95.02(9)
S(4)−Cu−S(1)	87.30(4)[e]	85.86(7)[e]	129.10(4)	112.15(9)
S(1)−Cu−S(3)	173.58(4)	170.15(7)	101.69(4)	121.91(8)
S(2)−Cu−S(4)	171.77(4)	168.48(6)	119.23(5)	123.18(10)
S(1)−Cu−O(1)	91.1(1)	92.4(2)		
S(2)−Cu−O(1)	93.6(1)	90.2(1)		
S(3)−Cu−O(1)	94.1(1)	96.8(2)		
S(4)−Cu−O(1)	93.7(1)	100.8(1)		

[a] For polymeric $Cu^{I}(L23)$, bond lengths and bond angles are based on the S(3)′ and S(4)′ atoms rather than S(3) and S(4) (see Figure 5). [b] For the corresponding $Cu^{II}(L2)(H_2O)$ cation, the Cu−O bond length is 2.18 Å and the mean Cu−S bond length is 2.32 Å (ref 9). [c] For the corresponding $Cu^{II}(L3)(H_2O)$ cation, the Cu−O bond length is 2.18 Å and the mean Cu−S bond length is 2.31 Å (ref 9). [d] For the corresponding $Cu^{I}(L3)$, the mean Cu−S bond length is 2.26 Å. [e] For both $Cu^{II}(L2)(H_2O)$ and $Cu^{II}(L3)(H_2O)$, the S(2)−Cu−S(3) and S(4)−Cu−S(1) bond angles are nearly equivalent (ref 9), whereas for $Cu^{II}(L23)$ and $Cu^{II}(L24)$, these two angles differ by 7° as shown.

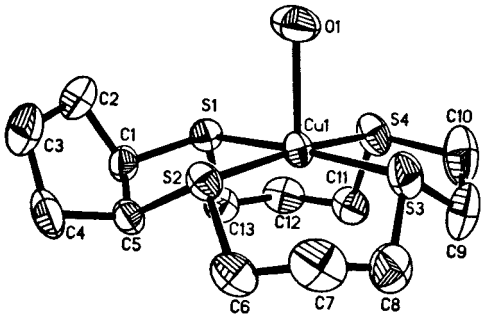

Figure 3. ORTEP diagram of the cationic unit of $Cu^{II}(L23)$ showing the atom labeling scheme. The Cu(II) is five-coordinate with the copper atom coordinated to all four sulfur donor atoms plus an apical water molecule. All lone pairs on the four donor atoms are pointed in the same direction relative to the apical water (conformer **I**) with the copper atom perched 0.13 Å above the average S_4 plane. Hydrogen atoms are omitted for clarity.

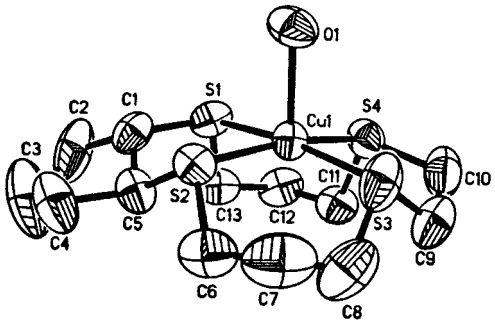

Figure 4. ORTEP diagram of the cationic unit of $Cu^{II}(L24)$ showing the atom labeling scheme. The Cu(II) is five-coordinate with the copper atom coordinated to all four sulfur donor atoms plus an apical water molecule. All lone pairs on the four donor atoms are pointed in the same direction relative to the apical water (conformer **I**) with the copper atom perched 0.20 Å above the average S_4 plane. Hydrogen atoms are omitted for clarity.

monomeric structure was obtained in which the Cu(I) atom is coordinated to all four sulfurs of a single ligand in a distorted tetrahedral geometry (Figure 6), similar to the structure previously resolved for $Cu^{I}(L3)$.[9] This structure is presumed to approximate the structures of both $Cu^{I}(L23)$ and $Cu^{I}(L24)$ as they exist in dilute solution.

Electron-Transfer Kinetics Studies. For both Cu(II/I) systems included in this work, an attempt was made to determine

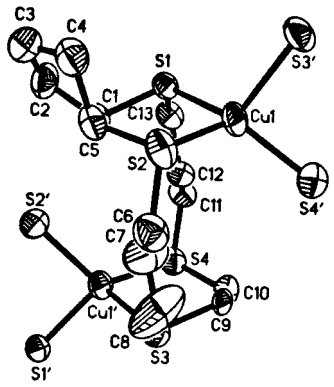

Figure 5. ORTEP diagram of the cationic unit of Cu^{I}(L23) showing a segment involving two tetrahedrally coordinated copper atoms bonded to the same macrocyclic ligand with the other two sulfur bonds to each copper from adjacent ligands. Hydrogen atoms are omitted for clarity.

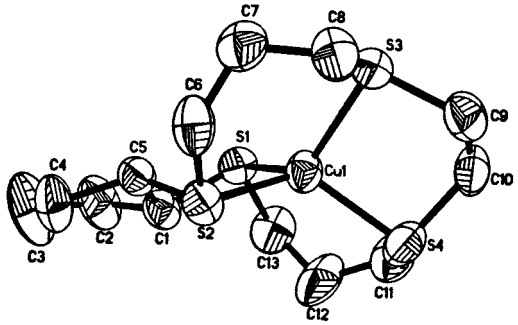

Figure 6. ORTEP diagram of the cationic unit of Cu^{I}(L24). The lone pairs on the sulfur donor atoms alternate direction relative to the macrocyclic ring (conformer **V**). Hydrogen atoms are omitted for clarity. A similar structure is presumed to be adopted by Cu^{I}(L23) in dilute solution.

the electron self-exchange rate constant, k_{11}, directly by NMR line-broadening measurements in D_2O with corrections for variable ionic strength as previously described.[32,33]

$$*Cu^{II}L + Cu^{I}L \overset{k_{11}}{\rightleftharpoons} *Cu^{I}L + Cu^{II}L \qquad (1)$$

For $Cu^{II/I}$(L23), reasonable plots were obtained yielding $k_{11} = (5 \pm 1) \times 10^4$ M^{-1} s^{-1} at 25 °C corrected to 0.10 M ionic strength (Table 4). Similar measurements for $Cu^{II/I}$(L24) proved unsatisfactory, presumably as a result of incomplete formation of the $Cu^{II}L$ complex due to its limited stability.

Each of the $Cu^{II}L$ complexes was reacted with three or four separate counter reductants ($Ru^{II}(NH_3)_5$py, $Ru^{II}(NH_3)_5$isn, $Ru^{II}(NH_3)_4$bpy, and $Ru^{II}(NH_3)_4$phen)[34] using stopped-flow spectrophotometry at 25 °C. A large excess of $Cu(ClO_4)_2$ was utilized to promote complete complexation, particularly in the case of Cu^{II}(L24). The corresponding $Cu^{I}L$ complexes were similarly reacted with three counter oxidants (selected among Ni^{III}([14]aneN$_4$), $Ru^{III}(NH_3)_4$bpy, $Ru^{III}(NH_3)_2$(bpy)$_2$, and Fe^{III}(4,7-Me$_2$phen)$_3$).[34] These reactions are represented as

$$Cu^{II}L + A_{Red} \overset{k_{12}}{\underset{k_{21}}{\rightleftharpoons}} Cu^{I}L + A_{Ox} \qquad (2)$$

where k_{12} and k_{21} are the second-order rate constants for $Cu^{II}L$ reduction and $Cu^{I}L$ oxidation, respectively, and A_{Red} and A_{Ox} represent the selected counter reagents. The formal potentials, electron self-exchange rate constants, and ion-size parameters applicable to all of the counter reagents utilized in this work have been given previously.[4,6,7]

Most of the $Cu^{II}L$ reduction reactions were studied under pseudo-first-order conditions in which the $Cu^{II}L$ concentration was present in at least 10-fold excess over the counter reagent concentration. For the fastest reactions, the two reactants were, at times, maintained at similar concentrations and the kinetics analyzed by a modified second-order approach that we have recently validated.[35] The kinetic runs for each set of reaction conditions were repeated approximately 10 times, and the results were averaged. The average rate constants for each set of runs are given in the Supporting Information. The resolved k_{12} and k_{21} values obtained for all cross reactions included in this investigation are listed in Table 4.

From past studies of related Cu(II/I) systems, we have noted that the oxidation reactions with Ni^{III}([14]aneN$_4$) may exhibit kinetic behavior that is either first order or zero order (or a mixture of both) with respect to the Ni(III) reagent depending upon the reagent concentration. Therefore, in the current study the Ni(III) reagent was maintained in large excess to generate pseudo-first-order conditions to ensure that uniform kinetic behavior was obtained for each single run. The apparent k_{21} values for both $Cu^{I}L$ species reacting with Ni^{III}([14]aneN$_4$) as a function of the Ni(III) concentration are available in the Supporting Information. In the specific case of the Cu^{I}(L24) oxidations with Ni^{III}([14]aneN$_4$), the pseudo-first-order rate constants became constant as the concentration of the Ni(III) reagent increased, indicating the onset of "gated" behavior. Further increases in the Ni(III) concentration resulted in the reappearance of the dependence of the pseudo-first-order rate constants on the concentration of the Ni(III) reagent. This behavior indicated a switch to the alternative reaction pathway as described in the Discussion.

Discussion

Properties of the Copper Complexes. The data in Table 1 show that the Cu(II) complexes with the two cyclopentane-substituted ligands (L23 and L24) differ in stability by about 75-fold. This is in sharp contrast to the behavior of the corresponding cyclohexane-substituted ligands (L2 and L3), which exhibit nearly equal $K_{Cu^{II}L}$ values. Since the calculated $K_{Cu^{I}L}$ values for the cyclopentane derivatives are equal (Table 1), it is evident that the high-potential value obtained for the L24 system is entirely due to the instability of its $Cu^{II}L$ complex.[25]

Evaluation of Self-Exchange Rate Constants. For each of the cross reactions studied, the Marcus relationship[36] (including both nonlinear and work term corrections) was applied to the experimental cross reaction rate constant (k_{12} or k_{21}) to permit the calculation of the apparent electron self-exchange rate constant (k_{11}) for the Cu(II/I) system as previously described (eq 1).[4,11] The resultant k_{11} values calculated for all reactions are listed as logarithmic values in Table 5.

In the specific case of the Cu^{I}(L24) oxidation reaction with Ni^{III}([14]aneN$_4$), the apparent k_{21} values change as a function

(32) Vande Linde, A. M. Q.; Juntunen, K. L.; Mols, O.; Ksebati, M. B.; Ochrymowycz, L. A.; Rorabacher, D. B. *Inorg. Chem.* **1991**, *30*, 5037−5042.

(33) Vande Linde, A. M. Q.; Westerby, B. C.; Ochrymowycz, L. A.; Rorabacher, D. B. *Inorg. Chem.* **1993**, *32*, 251−257.

(34) Ligand abbreviations are as follows: py = pyridine, isn = isonicotinamide, bpy = 2,2′-bipyridine, phen = 1,10-phenanthroline, [14]-aneN$_4$ = 1,4,8,11-tetraazacyclotetradecane (cyclam), 4,7-Me$_2$phen = 4,7-dimethyl-1,10-phenanthroline.

(35) Dunn, B. C.; Meagher, N. E.; Rorabacher, D. B. *J. Phys. Chem.* **1996**, *100*, 16925−16933.

(36) Marcus, R. A.; Sutin, N. *Biochim. Biophys. Acta* **1985**, *811*, 265−322.

Table 4. NMR Electron Self-Exchange and Cross Reaction Rate Constants for the Oxidation and Reduction of the Copper(II/I) Complexes with *cis*- and *trans*-cypt-[14]aneS$_4$ Reacting with Selected Counter Reagents in Aqueous Solution at 25 °C, $\mu = 0.10$

	k_{12} (or k_{21}) $\times 10^{-5}$, M^{-1} s^{-1}		calcd log k_{11}, M^{-1} s^{-1}	
counter reagent	*cis*-cypt-[14]aneS$_4$ (L23)	*trans*-cypt-[14]aneS$_4$ (L24)	*cis*-cypt-[14]aneS$_4$ (L23)	*trans*-cypt-[14]aneS$_4$ (L24)
NMR			4.7	*a*
reductants				
$Ru^{II}(NH_3)_4bpy$	4.4(3), 3.9(8), 3.5(2)	5.5(4)[b]	4.20, 4.09, 4.00	2.67
$Ru^{II}(NH_3)_4phen$		8.2(4)		3.12
$Ru^{II}(NH_3)_5isn$	15(1)	24(2)[b]	4.48	3.31
$Ru^{II}(NH_3)_5py$	33(3), 41(6)	58(4)	4.08, 4.27	3.07
oxidants				
$Ru^{III}(NH_3)_4bpy$	2.4(7)		3.67	
$Ni^{III}([14]aneN_4)(H_2O)$	22(2)	1.8 [A], 0.47 [B]	2.91	2.29 [A], 0.91 [B]
$Ru^{III}(NH_3)_2(bpy)_2$	6(1) $\times 10^2$	9.9(6)	2.80	0.59
$Fe^{III}(4,7\text{-}Me_2phen)_3$		58(3)		0.91
k_{RP},[c] s^{-1}	<0.002	0.0012(1)		

[a] NMR line-broadening measurements for $Cu^{II/I}$(L24) were unsatisfactory presumably because of the relative instability of the Cu(II) complex. [b] The pseudo-first-order rate constant data for the reduction of Cu^{II}(L24) (in excess) with $Ru^{II}(NH_3)_4bpy$ yielded a negative intercept. [c] The value of k_{RP} (the first-order rate constant for conformational change) for Cu^{I}(L24) was resolved from observed "gated" electron-transfer kinetics in the oxidation reaction by $Ni^{III}([14]aneN_4)$; the lower limit shown for Cu^{I}(L23) is based on the fact that no conformationally limited behavior was observed using the Ni(III) reagent.

Table 5. Comparative Self-Exchange Rate Constants for Pathways A and B and Rate Constants for the R → P Conformational Change for $Cu^{II/I}$(*cis*-cypt-[14]aneS$_4$) and $Cu^{II/I}$(*cis*-cypt-[14]aneS$_4$) and Related Systems in Aqueous Solution (Except As Specified) at 25 °C and $\mu = 0.10$ M

complexed ligand	log $k_{11(A)}$ (M^{-1} s^{-1})	log $k_{11(B)}$ (M^{-1} s^{-1})	log k_{RP} (s^{-1})	log ($k_{11(A)}/k_{11(B)}$)
[14]aneS$_4$ (L0)	3.88 ± 0.09[a]	−0.1 ± 0.2[a]	1.7 ± 0.1[a]	4.0
bz-[14]aneS$_4$ (L1)	2.9 ± 0.1[b]	0.7 ± 0.1[b]	≤−0.5[b]	2.2
cis-cyhx-[14]aneS$_4$ (L2)	4.7 ± 0.3[c]	∼1[c]	2.04 ± 0.02[c]	∼3.7
trans-cyhx-[14]aneS$_4$ (L3)	3.2 ± 0.2[c]	∼1[c]	1.51 ± 0.04[c]	∼2.2
cis-cypt-[14]aneS$_4$ (L23)	4.3 ± 0.2[d]	2.9[d]	<2.3[d]	1.4
trans-cypt-[14]aneS$_4$ (L24)	3.0 ± 0.3[d]	0.8[d]	2.1[d]	2.3

[a] Reference 4. [b] Value obtained in acetonitrile; ref 1. [c] Reference 9. [d] This work.

of the Ni(III) concentration. This behavior is characteristic for systems in which pathway A (Figure 1) is dominant under conditions where the R → P conformational change becomes rate-limiting. As we have noted earlier,[37] the complete expression for k_{21} for dual-pathway reactions is of the form[7]

$$k_{21} = \frac{k_{2A}k_{RP}}{k_{2A}[A_{Ox}] + k_{PR}} + k_{2B} \qquad (3)$$

where the two terms on the right represent the contributions of pathways A and B, respectively. At very low concentrations of $Ni^{III}([14]aneN_4)$, the contribution of the k_{2B} term to the Cu^{I}-(L24) oxidation appears to be negligible and $k_{2A}[A_{Ox}] \ll k_{PR}$ so that the kinetic data conform to the simple expression for second-order electron transfer via pathway A:

$$k_{21(A)} = k_{2A}K_{RP} \qquad (4)$$

where $K_{RP} = k_{RP}/k_{PR}$. At intermediate concentrations, the reaction becomes mixed first- and second-order because of the contribution of rate-limiting conformational change (k_{RP}), while at very high Ni(III) concentrations the k_{2B} term dominates and the reaction is again second order but with a different k_{21} value representative of reaction by pathway B. The changes in behavior are illustrated in Figure 7 where the two straight lines represent the regions of limiting second-order behavior. The value of k_{RP} can be evaluated from the data in the intermediate region using eq 3 as previously described.[1,4,7,9] Application of the Marcus cross relation to the two limiting k_{21} values permits the calculation of the apparent self-exchange rate constants for both pathways, i.e., $k_{11(A)}$ and $k_{11(B)}$. The resultant values are given in Table 4.

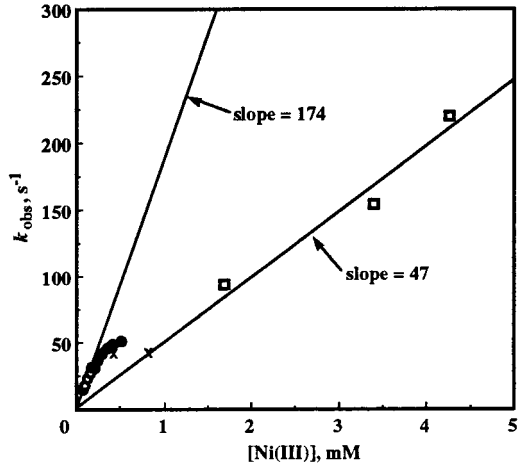

Figure 7. Plot of pseudo-first-order rate constants for the oxidation of Cu^{I}(L24) by $Ni^{III}([14]aneN_4)$ as a function of Ni(III) reagent concentration. The open circles represent limiting kinetics via pathway A at low Ni(III) concentrations for which $k_{21}(A) = 1.7 \times 10^5$ M^{-1} s^{-1} while the open squares represent limiting kinetics via pathway B for which $k_{21(B)} = 4.7 \times 10^4$ M^{-1} s^{-1}. The solid circles represent intermediate behavior in which the first-order conformational change R → P contributes to the overall electron-transfer rate, yielding $k_{RP} \approx 1 \times 10^2$ s^{-1}. The two points represented by "x" are out of line with the other data and were not included in the data resolution. (However, inclusion of these two points does not alter the results significantly.)

Interpretation of Resolved k_{11} Values. The data in Table 4 are listed in order of increasing driving force (as indicated by increasing k_{12} or k_{21} values) for both the oxidation and reduction

(37) Rorabacher, D. B.; Meagher, N. E.; Juntunen, K. L.; Robandt, P. V.; Leggett, G. H.; Salhi, C. A.; Dunn, B. C.; Schroeder, R. R.; Ochrymowycz, L. A. *Pure Appl. Chem.* **1993**, *65*, 573−578.

reactions. A comparison of the resolved k_{11} values obtained from the reduction kinetic studies of Cu^{II}(L23) shows that they are internally consistent and are in reasonable agreement with the k_{11} value obtained from the NMR line-broadening studies. Moreover, the oxidation reaction involving $Ru^{III}(NH_3)_4$bpy, which is thermodynamically uphill, yields a resolved k_{11} value that is also within acceptable agreement with the NMR and reduction values. However, the k_{11} values obtained from the oxidation kinetics carried out at higher driving force (with Ni^{III}-([14]aneN$_4$) and $Ru^{III}(NH_3)_2(bpy)_2$ as counter reagents) are approximately 1 order of magnitude smaller, indicating a probable switch in the reaction pathway. As we have noted earlier,[4,6,7,9] this pattern of behavior ($k_{11(red)} \geq k_{11(ox)}$) is characteristic of reactions in which the preferred reaction pathway is represented by pathway A, and for the fastest oxidation reactions, the cross reaction rate via pathway B exceeds the rate of conformational change (i.e., $k_{2B}[A_{Ox}] \gg k_{RP}$). Since limiting first-order kinetics were never observed for any of the Cu^{I}(L23) oxidation reactions, the specific value of k_{RP} cannot be evaluated accurately, but an upper limit has been established based on the conditions under which the switch to pathway B occurs.

The k_{11} values obtained for $Cu^{II/I}$(L24) show a similar pattern of behavior. However, as noted above, the oxidation kinetics for the reaction with Ni^{III}([14]aneN$_4$) did show a switch from second-order to first-order and back to second-order behavior as the Ni(III) concentration was increased so that $k_{21(A)}$, $k_{21(B)}$, and k_{RP} could all be evaluated for this cross reaction. The $k_{11(A)}$ value evaluated from this reaction is in reasonable agreement with the k_{11} values calculated from the three reduction reactions, and the $k_{11(B)}$ value obtained using the Ni(III) reagent is in agreement with the values obtained with the two oxidation reactions that exhibited higher driving force. Thus, all of the data for both $Cu^{II/I}$L systems are compatible with the dual-pathway square scheme mechanism in Figure 1 in which pathway A is preferred.

Comparison of Electron-Transfer Rate Constants to Related Copper(II/I) Systems. The most representative values for $k_{11(A)}$, $k_{11(B)}$, and k_{RP}, as obtained in the current study, are listed in Table 5 along with the corresponding values obtained for the closely related ligand systems illustrated in Figure 2. All of the data were acquired under identical conditions except for the $Cu^{II/I}$(L1) system, which was carried out in acetonitrile because of the insolubility of the ligand in aqueous solution. Previous studies have indicated that k_{11} and k_{RP} values for Cu(II/I) complexes of this type are virtually identical for these two solvents.[1,8] Therefore, we assume that the values for $Cu^{II/I}$(L1), acquired in acetonitrile, can be compared to the other values in aqueous solution.

Examination of the comparative rate constants in Table 5 reveals that the *cis*-cyhx-[14]aneS$_4$ (L2) (cyhx ≡ cyclohexanediyl) system studied previously[9] exhibits k_{11} values for both available pathways, which are about 1 order of magnitude larger than for the parent [14]aneS$_4$ (L0) system. By contrast, the *trans*-cyhx (L3) system reacts *more slowly* than the parent system by pathway A but *more rapidly* by pathway B. Almost identical behavior was noted for the bz-[14]aneS$_4$ (L1) system (bz ≡ benzene),[1] and the newly acquired data for the *trans*-cypt (L24) system yield nearly identical k_{11} values. However, the *cis*-cypt (L23) system exhibits a *significant decrease* in its reactivity via pathway A and a *very significant increase* in its reactivity via pathway B relative to its *cis*-cyhx (L2) analogue. In fact, $k_{11(B)}$ for the *cis*-cypt system is the largest self-exchange rate constant yet observed for this alternative pathway.

Conformational Changes Accompanying Copper(II/I) Electron Transfer. As shown in Figures 3 and 4 as well as in earlier structural determinations,[10,38,39] Cu(II) macrocyclic tetrathiaether complexes generally have all four sulfur donor atoms in virtually the same plane. However, the lone electron pairs on the coordinated sulfurs can be oriented either above (+) or below (−) the macrocyclic ring to generate five possible conformers. On the basis of their analogies to the *trans*-**I**, *trans*-**II**, etc. geometries previously defined for Ni^{II}([14]aneN$_4$),[40] these alternative conformations are designated as follows: conformer **I**, + + + +; conformer **II**, + − + +; conformer **III**, + − − +; conformer IV, + + − −; conformer V, + − + −.[10] A similar set of conformations exist for the Cu(I) complexes. (All 10 Cu^{II}L and Cu^{I}L conformers are illustrated in Figure S1 of the Supporting Information using the L3 system as an example.)

We have previously carried out semiquantitative molecular mechanical calculations on the various Cu^{II}L and Cu^{I}L conformers for the complexes with L0, L1, L2, and L3 using the MacSpartan Plus software (Wavefunction, Inc.) with the SYBYL force field option.[10] At that time we noted that qualitatively similar trends were obtained using the Chem3D Plus software package (version 3.0, Cambridge Scientific Computing, Inc., Cambridge, MA). In the current work, the latter calculations have been extended to include all conformers with the Cu(II) and Cu(I) complexes with L23 and L24 based on the expectation that differences in strain energies of the conformations might correlate with differences in kinetic behavior. For the purposes of comparison, chloride ions were placed in both axial positions for the calculations on the Cu^{II}L complexes. (The resulting "residuals", related to the remaining strain in the minimized geometry, as obtained using Chem3D Plus, are listed for all Cu^{II}L and Cu^{I}L conformers in Table S8 of the Supporting Information. Small differences in these "residuals" are not considered significant, particularly since Jahn−Teller distortion and solvation parameters are ignored in these calculations.)

All Cu(II) crystal structures reported for [14]aneS$_4$ (L0) and its derivatives[7,9,40] are either in conformer **I** or conformer **III**. From the molecular mechanical calculations, it is clear that the relative strain for both conformers is significantly greater for Cu^{II}(L24) than for the other Cu^{II}L complexes, particularly in the case of conformer **I**. We presume that this increased strain accounts for the notably smaller $K_{Cu^{II}L}$ stability constant observed for the Cu^{II}(L24) complex (Table 1). (By contrast, the huge reduction in $K_{Cu^{II}L}$ for Cu^{II}(L1) is attributed to the negative inductive effects of the benzene ring rather than to inherent strain.) In the case of the corresponding Cu^{I}L species, both the molecular mechanical calculations (Table S8) and recent crystal structures (e.g., Figure 6)[9] indicate that the most stable conformer is conformer V (+ − + −) in all cases.

On the basis of the crystallographic and molecular mechanical data, it is apparent that electron transfer in these Cu(II/I) macrocyclic ligand systems must involve the inversion of two donor atoms regardless of whether the Cu^{II}L species exists in

(38) Glick, M. D.; Gavel, D. P.; Diaddario, L. L.; Rorabacher, D. B. *Inorg. Chem.* **1976**, *15*, 1190−1193.
(39) Pett, V. B.; Diaddario, L. L., Jr.; Dockal, E. R.; Corfield, P. W.; Ceccarelli, C.; Glick, M. D.; Ochrymowycz, L. A.; Rorabacher, D. B. *Inorg. Chem.* **1983**, *22*, 3661−3670.
(40) Bosnich, B.; Poon, C. K.; Tobe, M. L. *Inorg. Chem.* **1965**, *4*, 1102−1108. The *trans* terminology adopted by Bosnich, Poon, and Tobe for Ni^{II}([14]aneN$_4$) complexes refers to the fact that the remaining two coordination sites are trans to each other. Although the trans designation is not applicable to five-coordinate Cu^{II}L complexes or four-coordinate Cu^{I}L complexes, the same numbering scheme can be utilized for the various conformers based on the orientation of the lone electron pairs relative to the macrocyclic ring.

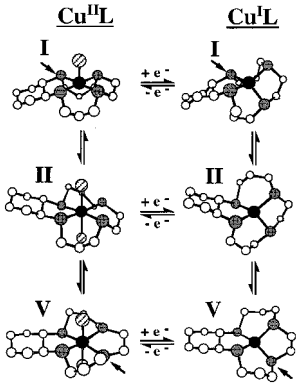

Figure 8. Proposed three-rung ladder scheme for Cu(II/I) electron transfer involving [14]aneS$_4$-type complexes (adapted from ref 10). The *trans*-dicyhx-[14]aneS$_4$ (L3) system is utilized in these representations. Vertical reactions represent conformational changes. while horizontal reactions involve electron transfer (rate constants omitted for simplicity). The stable form of Cu^{II}L is represented here by conformer **I**, but for other macrocycles either conformer **I** or **III** could predominate. It is hypothesized that conformers **I** and **II** of Cu^{II}L are in rapid equilibrium and, together, represent species O in Figure 1. Species P, Q, and R in Figure 1 are then presumed to represent conformers Cu^{I}L(II), Cu^{II}L-(V), and Cu^{I}L(V), respectively (see text).

conformer **I** or **III**. As we have noted earlier,[10] the conversion of conformer **I** or **III** to conformer **V** must always involve conformer **II** as an intermediate species (see Figure S1 of the Supporting Information). (Conformer IV represents a "dead end" and, therefore, is of no specific interest.) If the most stable Cu^{II}L geometry is represented by conformer **I**, there are three available pathways for electron transfer as illustrated in Figure 8. On the basis of the molecular mechanical calculations, conformer **II** would appear to be the most favorable intermediate for both Cu^{II}L and Cu^{I}L. Thus, in the absence of other considerations, we presume that the preferred reaction pathway is Cu^{II}L(I) $\rightleftharpoons$ Cu^{II}L(II) $\rightleftharpoons$ Cu^{I}L(II) $\rightleftharpoons$ Cu^{I}L(V). If this sequence represents pathway A, Cu^{II}L(I) and Cu^{II}L(II) must be in rapid equilibrium and, together, represent species Cu^{II}L(O) in Figure 1. Similarly, Cu^{II}L(Q), Cu^{I}L(P), and Cu^{I}L(R) must then coincide with conformers Cu^{II}L(V), Cu^{I}L(II), and Cu^{I}L(V). These conclusions imply that conformer **I** for Cu^{I}L—in the upper right corner of Figure 8—does not contribute significantly to the overall reaction kinetics. (This conclusion is consistent with the calculated relative strain energies listed in Table S8 of the Supporting Information.)

Unfortunately, a comparison of the molecular mechanical calculations with the rate constant data in Table 5 fails to provide significant correlations. Whereas the Cu(II/I) system involving the *trans*-cyhx derivative (L3) exhibits a $k_{11(A)}$ value that is one and one-half orders of magnitude smaller than its *cis* analogue (L2), the relative strain energies for the various conformers of these two systems are nearly identical. For the corresponding cyclopentanediyl derivatives, nearly all conformers of the *trans*-cypt system (L24) exhibit significantly higher strain energies, yet both the $k_{11(A)}$ and $k_{11(B)}$ values are similar to that of the corresponding *trans*-cyhx (L3) system.

In an attempt to improve upon the strain calculations, we have carried out extensive *ab initio* calculations on the conformers of the L0 system using Gaussian 99 at the HF/LANL2DZ level of theory.[41] For reasons as yet unidentified, the results to date are less satisfactory than those obtained from the more approximate molecular mechanical calculations. We conclude that the lack of correlation between our qualitative strain energies and the kinetic rate constants is primarily due to the fact that the conformational calculations represent only the stable or metastable species while no information is available on the strain energies of the transition states.

Conclusions

The replacement of an ethylene bridge in [14]aneS$_4$ by benzene, cyclohexane, or cyclopentane is observed to modify the electron-transfer kinetics of the Cu(II/I) complexes. For both the cyclohexanediyl and cyclopentanediyl derivatives of [14]-aneS$_4$, the *cis* enantiomers increase the Cu$^{II/I}$L $k_{11(A)}$ value whereas the *trans* enantiomers, as well as the phenylene derivative, result in a significant decrease relative to the parent L0 system. All five derivatized systems result in increased values of $k_{11(B)}$ relative to Cu$^{II/I}$(L0), and this effect is particularly dramatic in the case of the *cis*-cypt derivative (L23), which exhibits the largest $k_{11(B)}$ value yet observed for a macrocyclic tetrathiaether. In fact, the k_{RP} value for this last system could not be evaluated from the oxidation kinetics with Ni^{III}([14]-aneN$_4$) because of the surprisingly large $k_{11(B)}$ value.

In the case of the Cu$^{II/I}$(*trans*-cypt-[14]aneS$_4$) (L24) system, molecular mechanical calculations indicate that all conformers are significantly more strained than for the other systems listed. The increased strain for the Cu(II) complex in conformer **I** doubtless accounts for the much smaller Cu^{II}L stability constant obtained for this system. However, this strain is not reflected in the electron-transfer kinetics relative to the behavior of the corresponding *trans*-cyhx derivative (L3). From these and related observations made in conjunction with the current study, we conclude that the energetics of accessing the relevant transition states are not directly reflected in the relative strain energies of the ground state and the metastable intermediates. However, the molecular mechanical calculations do suggest that the metastable intermediates identified as Cu^{II}L(Q) and Cu^{I}L-(P) in our original square scheme dual-pathway mechanism are likely to represent conformer **V** of Cu^{II}L and conformer **II** of Cu^{I}L, respectively, for this series of macrocyclic ligands.

Acknowledgment. This work was supported by the National Science Foundation under Grants CHE-9528831 and CHE-9817919.

Supporting Information Available: Tables of experimental cross reaction rate constants and molecular mechanical residual strain energies, an illustration of the major conformers for Cu^{I}L and Cu^{II}L complexes, and four X-ray crystallographic files in CIF format. This material is available free of charge via the Internet at http://pubs.acs.org.

IC0000909

(41) Kropfreiter, D.; Schlegel, H. B.; Rorabacher, D. B. Unpublished results.